

 Open access • Proceedings Article • DOI:10.1109/VLSIC.2014.6858425

A millimeter-scale wireless imaging system with continuous motion detection and energy harvesting — [Source link](#)

Gyouho Kim, Yoonmyung Lee, Zhiyoong Foo, Pat Pannuto ...+10 more authors

Institutions: University of Michigan

Published on: 10 Jun 2014 - Symposium on VLSI Circuits

Topics: Photovoltaic system, Energy harvesting, Motion detection and Image sensor

Related papers:

- [A Modular 1 mm \$3 \times 3\$ Die-Stacked Sensing Platform With Low Power \$1 \times 1\$ C Inter-Die Communication and Multi-Modal Energy Harvesting](#)
- [A Portable 2-Transistor Picowatt Temperature-Compensated Voltage Reference Operating at 0.5 V](#)
- [Circuits for a Cubic-Millimeter Energy-Autonomous Wireless Intraocular Pressure Monitor](#)
- [A Fully-Integrated 71 nW CMOS Temperature Sensor for Low Power Wireless Sensor Nodes](#)
- [A cubic-millimeter energy-autonomous wireless intraocular pressure monitor](#)

Share this paper:    

View more about this paper here: <https://typeset.io/papers/a-millimeter-scale-wireless-imaging-system-with-continuous-3j8ac49uq3>

A Millimeter-Scale Wireless Imaging System with Continuous Motion Detection and Energy Harvesting

Gyouho Kim, Yoonmyung Lee, Zhiyong Foo, Pat Pannuto, Ye-Sheng Kuo, Ben Kempke, Mohammad Hassan Ghaed, Suyoung Bang, Inhee Lee, Yejoong Kim, Seokhyeon Jeong, Prabal Dutta, Dennis Sylvester, David Blaauw

University of Michigan, Ann Arbor, MI

Abstract

We present a $2\times4\times4\text{mm}^3$ imaging system complete with optics, wireless communication, battery, power management, solar harvesting, processor and memory. The system features a 160×160 resolution CMOS image sensor with 304nW continuous in-pixel motion detection mode. System components are fabricated in five different IC layers and die-stacked for minimal form factor. Photovoltaic (PV) cells face the opposite direction of the imager for optimal illumination and generate 456nW at 10klux to enable energy autonomous system operation.

Introduction

Visual imaging is a highly desired feature for wireless sensing applications such as biological monitoring and surveillance. Recent advances in low power circuit techniques and integration have resulted in self-sustaining wireless sensor nodes as small as 1mm^3 [1-3]. However, achieving a complete visual sensing system in a similar volume is challenging due to physical difficulties in integrating optics and the high power consumption of key components such as the image sensor and RF transmitter. This work introduces a millimeter-scale wireless sensor node with visual imaging and ultra-low power motion detection. The overall system sleep power is 304nW with motion detection enabled, allowing energy-autonomous operation with 10klux of background lighting, which is a typical daytime condition on a window or light source surface. The system also features on-demand duty-cycling, in which the system wakes up when triggered by motion to capture an image and can restrict the read out to the portion of the image where motion was detected.

Proposed System

Fig. 1 shows pictures and a cross-sectional diagram of the proposed system. The glass package with vias provides a connection between the top-facing chips and bottom-facing PV cells. This configuration creates optimal lighting conditions for both imaging and harvesting. Transparent protective epoxy covers the PV cells and bond wires below the glass package. A gradient-index (GRIN) rod lens is used for optics, measuring 1mm in diameter and 2.4mm in height. The lens is mounted on the surface of the image sensor with UV-curable optical epoxy. Since the ultra-low power circuits in the system exhibit high leakage when exposed to strong light, the cavity inside the glass package is filled with dark epoxy to shield non-imaging chips from light and complete the encapsulation.

Fig. 2 outlines the major system components. A new unidirectional, fully synthesizable inter-layer communication bus (Mbus) is introduced, designed specifically for ultra-low power and robust operation. Mbus master and slave layers are arranged in a daisy chain topology. The processor (PRC) layer generates Mbus clock as the master layer and also contains an ARM M0 core and 3kB SRAM. The Mbus clock wires toggle only when there is bus activity, minimizing the active power. An Mbus layer is either in forwarding (default) or issuing mode. In the default mode, C_{IN}/D_{IN} are directly forwarded to C_{OUT}/D_{OUT} , which 1) allows accurate synchronization of layers since delay through the daisy chain is small and deterministic, and 2) removes the need for a local clock on each layer, minimizing the power overhead of adding layers to the loop.

One key feature of Mbus is its interrupt generation during system sleep mode. The power management unit (PMU) in the PRC layer provides 1.2V and 0.6V power domains, down-converted from the 3.8V battery voltage. The PMU can sustain 10-100nA load on both supplies during sleep mode and up to 50 μ A during active mode. The system can wake up from sleep mode either via a built-in wake-up timer in the PRC layer or by interrupts generated by slave layers that operate in sleep mode, e.g., motion detection. To issue this interrupt, the slave must initiate an Mbus message to the PRC while staying within the extremely low power budget of standby mode. To this end, Mbus data wires use a high default state and a message request is performed by pulling down on this wire, which is forwarded to the master, and consumes near-zero energy. The PMU then switches to active mode and all Mbus layers wake up, allowing the remainder of the message to be sent. An added benefit of this approach is that only the sleep and wire controllers remain powered on during sleep mode (Fig. 3), resulting in Mbus sleep power of 6pW per layer.

To allow flexible message length while using only two wires, end-of-message (EOM) is encoded by holding clock high while the data

toggles three times (detection circuit shown in Fig. 4). The EOM detector is also used to allow message interrupt. When a layer issues an interrupt while the Mbus is already active, it blocks the incoming clock (C_{OUT} held high), which is then recognized by the Mbus master. The master then sends the EOM sequence, allowing the interrupting layer to gain control.

The image sensor in the IMG layer produces 8/9-bit 160×160 resolution images with cropping and row/column skipping features to reduce data bandwidth and storage. Motion detection pixels of 10×10 resolution are built-in to the array (Fig. 6), with temporal averaging to improve detection sensitivity to slow motions [4]. For motion detection, pixel values of the previous frame are stored on C_{HOLD} , which is distributed in the motion detection cluster of 16×16 pixels, achieving pixel size of $5.4\times5.4\mu\text{m}^2$ and 37% fill factor. At the end of an integration cycle, both the current and previous pixel values are read out and compared (Fig. 7). A 14-level configurable detection threshold is used to determine if the inter-frame pixel difference is large enough to be flagged as motion. A new bootstrapping circuit is designed to eliminate reset hysteresis for boosted row control signals (Fig. 8). In the conventional cross-coupled design, node $n1$ does not fully charge up to VDD in steady state, resulting in a different initial boosted voltage in pulsed signal sequence. The proposed single-ended design uses NMOS with its body tied to VDD to lower V_{th} , raising $n1$ to full VDD when input A is 0.

In the ultra-low power motion detection mode, pixels and ADC for full-frame imaging are hierarchically power-gated (Fig. 9), and motion detection is performed at 5×5 resolution. Since image readout consumes up to 1mA instantaneous current, 100pF decoupling capacitance is added for each power-gated domain. To prevent power rail collapse when initially enabling the large capacitors, a smaller assistive power gating device is implemented that turns on before the main power gating device. To reduce leakage power of 0.6V digital components, N-wells are biased at 1.2V, reducing PMOS leakage by $60\times$ in simulation.

Frame-wise thresholding of motion trigger count is implemented to prevent against false triggers or dead pixels. The location of the motion detecting pixel is also reported, which can be used to determine which portions of the image to store in SRAM. Fig. 5 shows state changes of each layer and Mbus activity for one of the tested usage scenarios of motion-triggered system wakeup and RF transmission.

Two-way wireless communication is achieved with optical wakeup receiver and RF transmitter. The optical receiver [5] consumes 695pW standby power and is used to initially load the program and to request data. The RF transmitter uses an OOK-modulated scheme, with an LC oscillator tuned to the 915MHz ISM band. The oscillator is turned on for 100ns to transmit 1 bit and is otherwise power-gated.

Measurement Results

Five of the proposed imaging system were assembled with 80% yield and demonstrated full functionality. The glass package with bottom facing PV cells is first assembled and placed on a glass slide. The battery and IC layers are then stacked and wirebonded, and finally the lens is mounted. With the 5.7 μ Ah thin-film battery, the system can survive up to 60 days in a 4nA sleep mode or perform continuous motion detection for 3.4 days consuming 80nA from the 3.8V battery. With 10klux illumination, battery charging by the PMU at 120nA was observed, which is sufficient to sustain continuous motion detection operation. Fig. 10 shows measured battery current as the system wakes up upon motion, transmits data, and returns to sleep. Image sensor SNR in its 9-bit configuration is 47dB (Fig. 11). The RF transmitter in the stack sends data at 4nJ/bit to an inductive receiver with -70dBm of sensitivity positioned 15mm away. Fig. 12 shows die photos of the three key IC layers.

Acknowledgement

The authors thank Cymbet Corporation for supplying the battery and Advotech Company for close collaboration on the assembly process.

References

- [1] E. Chow *et al.*, *ISSCC* 2010.
- [2] G. Chen *et al.*, *ISSCC*, 2011.
- [3] Y. Lee *et al.*, *ISSCC*, 2012.
- [4] G. Kim *et al.*, *ISSCC*, 2013.
- [5] G. Kim *et al.*, *CICC*, 2012.
- [6] C. Park *et al.*, *SenSys*, 2006.
- [7] INCA, *Fraunhofer Press Release*, December 2011.

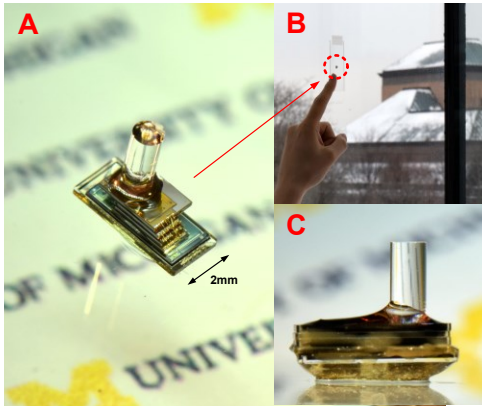


Figure 1. The proposed imaging system on a raised glass slide (a) is nearly invisible when mounted on a window (b). Glass sidewalls and dark epoxy filling completely encapsulates the system and prevents light-induced leakage current (c). Cross sectional diagram of the system is shown on the right.

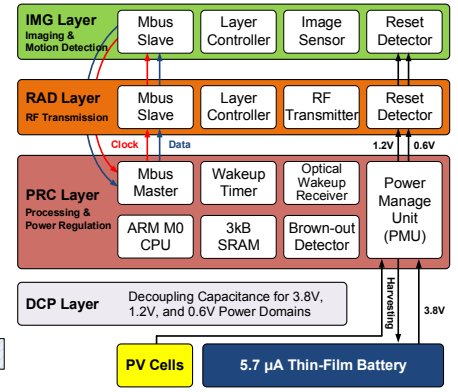
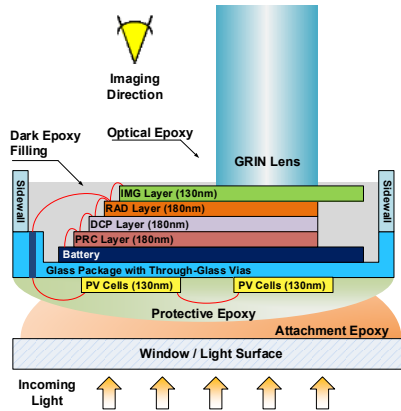


Figure 2. System block diagram showing key components in each IC layer. Mbus is used for robust and low-power inter-layer communication.

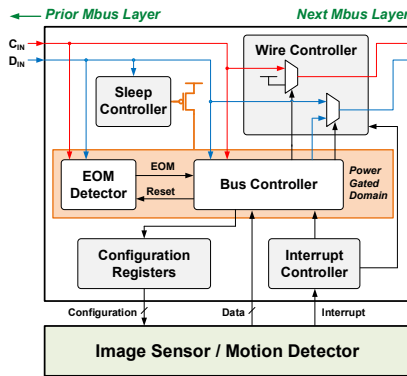


Figure 3. Block diagram of Mbus components shown for IMG layer as an example.

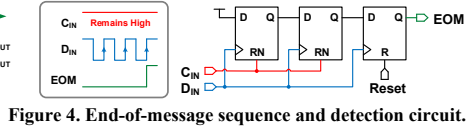


Figure 4. End-of-message sequence and detection circuit.

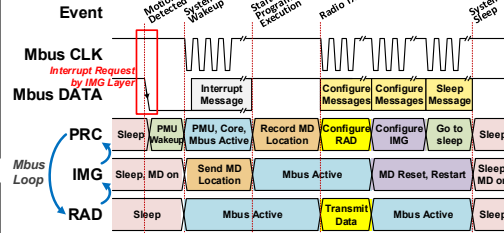


Figure 5. Mbus timing diagram and layer status during motion-triggered system wakeup and radio transmission.

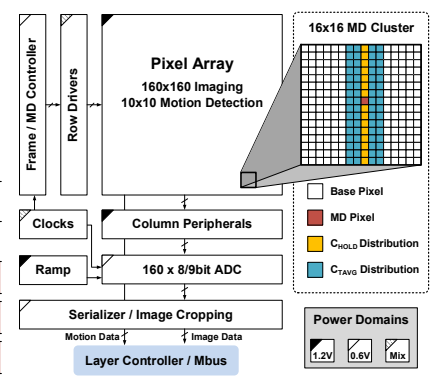


Figure 6. Block diagram of the image sensor with in-pixel motion detection and arrangement of pixels.

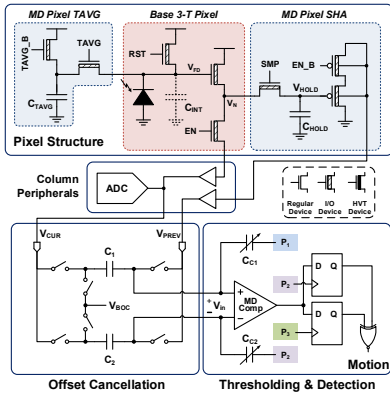


Figure 7. Pixel structure and column readout scheme for imaging and motion detection.

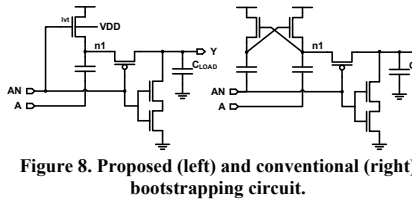


Figure 8. Proposed (left) and conventional (right) bootstrapping circuit.

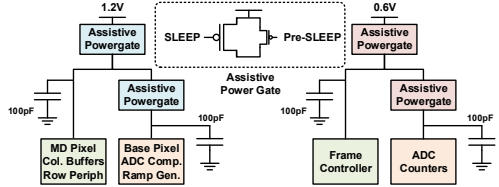


Figure 9. Hierarchical power gating scheme of image sensor and assistive power gate structure.

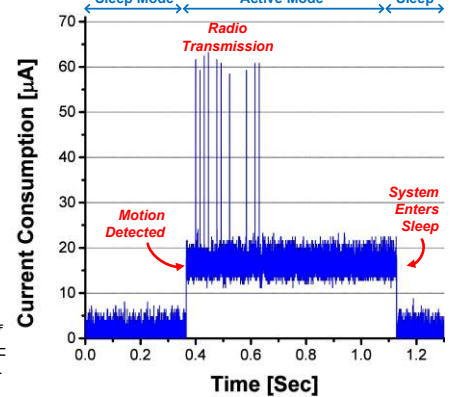


Figure 10. Measured current drawn from the battery, showing system wakeup triggered by motion.



Figure 11. Sample image taken with the image sensor and GRIN lens, transmitted via Mbus.

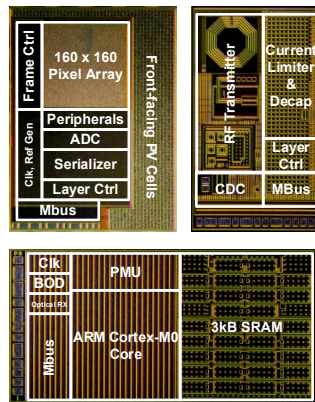


Figure 12. Die photos of IMG, RAD, and PRC layers (from top left, clockwise).

Categories	Wireless Sensor Nodes		This Work	Miniaturized Cameras	
	IOP [2]	M3 [3]		eCAM [6]	INCA [7]
Imaging	N/A	9,216 Pixels	25,600 Pixels w/ Motion Detection	0.3 MPixels	2 MPixels
Optics	N/A	N/A	GRIN Rod Lens	Pinhole Lens	Regular Lens
Wireless	RF Transceiver	Optical Receiver	Optical Receiver RF Transmitter	2.4GHz Transceiver	LTE Module Optional
Processor	ARM Cortex M0	ARM Cortex M0	ARM Cortex M0	Nordic 8051	TI OMAP 4
Storage	0.5kB SRAM	3kB SRAM	3kB SRAM	4kB SRAM	Unknown
Battery Capacity	1μAh Thin-Film	1μAh Thin-Film	5.7μAh Thin-Film	170mAh Li-Poly	No Battery
Standby Power	3.7nW	11nW	15nW idle, 304nW with MD	At least 100μW	4W
Energy Harvesting	Solar, 0.07mm ²	Solar, 0.54mm ²	Solar, 2.5mm ²	N/A	N/A
System Lifetime	Perpetual	Perpetual	Perpetual	<240days	Wired
Dimensions	0.5 × 1.5 × 2 mm ³	1 × 2.2 × 0.4 mm ³	2 × 4 × 4 mm ³	23 × 32 × 18 mm ³	20 × 20 × 80 mm ³

Table 1. Comparison table of proposed visual sensing system against wireless sensor nodes and miniaturized cameras.